

RESEARCH ARTICLE

Analysis of secondary metabolite gene clusters and chitin biosynthesis pathways of *Monascus purpureus* with high production of pigment and citrinin based on whole-genome sequencing

Song Zhang¹, Xiaofang Zeng², Qinlu Lin¹, Jun Liu^{1,3*}

1 National Engineering Research Center of Rice and Byproduct Deep Processing, Central South University of Forestry and Technology, Changsha, Hunan, China, **2** College of Light Industry and Food Sciences, Zhongkai University of Agriculture and Engineering, Guangzhou, Guangdong, China, **3** Hunan provincial Key Laboratory of Food Safety Monitoring and Early Warning, Changsha, Hunan, China

* liujundandy@csuft.edu.cn**OPEN ACCESS**

Citation: Zhang S, Zeng X, Lin Q, Liu J (2022) Analysis of secondary metabolite gene clusters and chitin biosynthesis pathways of *Monascus purpureus* with high production of pigment and citrinin based on whole-genome sequencing. PLoS ONE 17(6): e0263905. <https://doi.org/10.1371/journal.pone.0263905>

Editor: Minou Nowrouzian, Ruhr-Universitat Bochum, GERMANY

Received: January 17, 2022

Accepted: April 25, 2022

Published: June 1, 2022

Peer Review History: PLOS recognizes the benefits of transparency in the peer review process; therefore, we enable the publication of all of the content of peer review and author responses alongside final, published articles. The editorial history of this article is available here: <https://doi.org/10.1371/journal.pone.0263905>

Copyright: © 2022 Zhang et al. This is an open access article distributed under the terms of the [Creative Commons Attribution License](https://creativecommons.org/licenses/by/4.0/), which permits unrestricted use, distribution, and reproduction in any medium, provided the original author and source are credited.

Data Availability Statement: All relevant data are within the paper and its [Supporting Information](#) files.

Abstract

Monascus is a filamentous fungus that is widely used for producing *Monascus* pigments in the food industry in Southeast Asia. While the development of bioinformatics has helped elucidate the molecular mechanism underlying metabolic engineering of secondary metabolite biosynthesis, the biological information on the metabolic engineering of the morphology of *Monascus* remains unclear. In this study, the whole genome of *M. purpureus* CSU-M183 strain was sequenced using combined single-molecule real-time DNA sequencing and next-generation sequencing platforms. The length of the genome assembly was 23.75 Mb in size with a GC content of 49.13%, 69 genomic contigs and encoded 7305 putative predicted genes. In addition, we identified the secondary metabolite biosynthetic gene clusters and the chitin synthesis pathway in the genome of the high pigment-producing *M. purpureus* CSU-M183 strain. Furthermore, it is shown that the expression levels of most *Monascus* pigment and citrinin clusters located genes were significantly enhanced via atmospheric room temperature plasma mutagenesis. The results provide a basis for understanding the secondary metabolite biosynthesis, and constructing the metabolic engineering of the morphology of *Monascus*.

Introduction

Fermented products of *Monascus* spp. have been widely used in the food and pharmaceutical industry for more than 2000 years [1]. As the secondary metabolite produced by *Monascus* spp., *Monascus* pigments (MPs) are a mixture of azaphilones mainly composed of three colors (yellow, orange, and red) pigments, which possess various bioactivities, such as antimicrobial, anticancer, anti-inflammatory, and anti-obesity [2, 3]. Nowadays, due to the potential risks of allergies, carcinogenesis, and teratogenesis of synthetic pigments, natural MPs are widely used

Funding: This work was supported by the National Natural Science Foundation of China (No. 32101906), Natural Science Foundation of Hunan Province (No. 2021JJ31146); Open Project Program of the Hunan Provincial Key Laboratory of Food Safety Monitoring and Early Warning (No. 2021KFJJ02), Education Department of Scientific Research Project of Hunan Province (No. 20B619) and Education Department of Postgraduate Research and Innovation Project of Hunan Province (No. CX20210863. The funders had no role in study design, data collection and analysis, decision to publish, or preparation of the manuscript.

Competing interests: The authors have declared that no competing interests exist.

as food colorants and are well recognized by consumers [4, 5]. In addition, MPs have other applications in the pharmaceutical, textile, and cosmetics industries. Traditionally, MPs are mainly produced by solid-state fermentation (SSF) with rice as the substrate for high pigment concentration [6]. However, submerged fermentation (SF) was more widely applied in the industrial production at present due to high pigment production efficiency, an easy-to-control fermentation process, and avoidance of contamination [7, 8].

Different species of *Monascus* spp. have been isolated for the biosynthesis of various secondary metabolites. In general, *M. fuliginosus* [9, 10], *M. ruber* [11, 12] and *M. pilosus* [13–15] have a strong capacity to produce monacolin K. Nevertheless, *M. purpureus* is the most predominant microorganisms for the efficient production of MPs because of its high efficiency to produce pigments [16–18]. With the development of whole-genome sequencing (WGS) technology, the complete sequence analysis of *Monascus* has been used to reveal the chromosome evolution, regulatory mechanisms, and functional genes of *M. purpureus*, which lays the foundation for the production of secondary metabolites and biological researches. In 2015, Yang et al. published the first sequence information of *M. purpureus* YY-1, with a genome size of 24.1 Mb and a total of 7491 predicted genes. WGS analysis predicted the gene clusters related to pigment biosynthesis in *M. purpureus* YY-1 and explained the smaller size of the *M. purpureus* genome than that of related filamentous fungi, indicating a significant loss of genes [19]. Kumagai et al. reported the genome sequence information of the high pigment-producing *M. purpureus* GB-01 strain, with a genome size of 24.3 Mb and 121 chromosomal contigs [20]. Liu et al. identified the key genes (*ERG4A* and *ERG4B*) for ergosterol biosynthesis in *M. purpureus* LQ-6 (genome size: 26.8 Mb, 8596 protein-coding genes). Knocking out the *ERG4* gene improved the permeability of the cell membrane and secretion of intracellular pigments; it also changed the morphology of *M. purpureus* LQ-6 in SF broth [21]. Although numerous studies on the morphological changes of *Monascus* in SF have been performed, the biological information on the metabolic engineering of morphology of *Monascus* remains unknown [22–24].

Hyphae of filamentous fungi in SF mainly exist in three morphological forms, including free mycelia, mycelial pellets, and mycelial clumps [25], and the difference of metabolites is probably due to the different morphology of hyphae. The mycelium pellet is the optimal morphology for glucoamylase production by *Aspergillus niger*, while the fermentation production of citric acid is more biased to the mycelial morphology [26]. The *veA* gene globally regulates the propagation mode, mycelial growth, environmental tolerance, and secondary metabolites of fungi [27, 28]. Muller et al. disrupted the biosynthesis of chitin and changed the morphology of *Aspergillus oryzae* by regulating the transcription level of the chitin synthase gene *chsB*, and studied the relationship between morphology and α -amylase biosynthesis [29]. RNA interference technology has been applied to silence the expression of the chitin synthase gene *chs4* in *Penicillium chrysogenum*, reducing the mutant growth rate, aggregation of dispersed hyphae into the mycelium, and increased penicillin production [30]. With the in-depth study of different phenotype mutants, it is found that the cell wall is an ideal target for morphological control. However, the differences were existed in the encoding genes of chitin synthase and the regulation of chitin synthase on morphology in different fungi [31]. Furthermore, the specific encoding genes of chitin synthase and biosynthesis pathway of chitin in *M. purpureus* is still unclear.

M. purpureus CSU-M183 is a high pigment-producing industrial preparation strain obtained by atmospheric room temperature plasma (ARTP) mutation system. In this study, the whole genome of strain CSU-M183 was sequenced using the single-molecule real-time (SMRT, PacBioRS II) DNA sequencing and Illumina next-generation sequencing (NGS) platforms. We also investigated the molecular expression effects of ARTP mutagenesis on the secondary metabolic synthesis of *Monascus* by RT-qPCR. The results showed a comprehensive

prediction of biosynthetic gene clusters (BGCs) for secondary metabolites and the biosynthetic pathway of chitin in *M. purpureus* CSU-M183. We expect this will provide a better strategy in morphological metabolic engineering of *Monascus*, for the industrial production of the secondary metabolites via submerged fermentation.

Materials and methods

Fungal strains, culture media, and growth conditions

M. purpureus CSU-M183 (CCTCC M 2018224, China Central for Type Culture Collection (CCTCC), Wuhan, China) was obtained using the ARTP mutation system from the parent strain *M. purpureus* LQ-6 (CCTCC M 2018600) [32]. Strains was cultivated on potato dextrose agar (PDA) and potato dextrose broth (PDB) medium at 30°C in the dark for 7 days.

To prepare the inoculum, spores were transferred from PDA slants to submerged culture medium and washed with sterile distilled water, and then diluted to approximately 3×10^7 spores/ml. The 10% (v/v) inoculum was transferred to the submerged culture medium and incubated 7 days. 10% (V/V) of the inoculum was transferred to 250 ml shark flasks containing 45 ml liquid medium and incubated for 7 days in a rotary shaker with parameters set at 30°C and 180 rpm, respectively.

DNA extraction

Mycelia were collected after centrifugation at $8228 \times g$ for 10 min and stored at -80°C . Genomic DNA was extracted from mycelia using the *EasyPure*[®] Genomic DNA Kit (TransGen Biotech, Beijing, China) according to the manufacturer's protocol. The quantity, quality, and purity of the genomic DNA were measured using Nanodrop2000 systems and 0.8% DNase-free agarose gel electrophoresis.

WGS and assembling

The whole genome of the *M. purpureus* CSU-M183 strain was sequenced using SMRT sequencing technology of PacBioRS II, and the sequencing quality was improved using Illumina NGS platform. The sequencing library was constructed using the TruSeq[™] Nano DNA LT Sample Prep Kit-Set A (Illumina, USA) and amplified using the TruSeq PE Cluster Kit (Illumina, USA).

The quality of the assembled genome and annotated geneset were assessed first using the Benchmarking Universal Single-Copy Orthologs (version 3.1.0; BUSCO) with the fungi_odb9 dataset [33].

For raw data polymerase reads after PacBioRS II sequencing, subreads were obtained by removing the low-quality or unknown reads, adapters and duplications. The filtered reads were assembled *de novo* using the Hierarchical Genome Assembly Process (HGAP) algorithm version 2.0 [34].

For genome assembly, the default parameters of HGAP2 were used (Minimum Subread Length = 500, Minimum Polymerase Read Quality = 0.80, Minimum Polymerase Read Length = 100, Overlapper Error Rate = 0.06, Overlapper Min Length = 40) with input genome size as 30 Mb.

PacBio library construction. High-quality DNA (10 µg in 200 µl 10 mM Tris-HCl pH8.5) was sheared using a Covaris g-tube (Covaris Inc.) with 6000RPM for 60seconds. Sheared DNA was purified by binding to 0.45X volume of pre-washed AMPure XP beads (Beckman Coulter Inc.), and eluted in EB to >140 ng/µl. The sheared DNA was quantified on an Agilent 2100 Bioanalyzer using the 12000 kit. 5 µg of sheared DNA was end-repaired using

the PacBio DNA Template Prep Kit 2.0 (Part Number 001-540-835) and incubated for 20 min at 37°C and then 5 min at 25°C prior to another 0.45X AMPure XP clean up, eluting in 30 µl EB. Blunt adapters were ligated before exonuclease incubation. Finally, two 0.45X AMPure bead clean ups are performed to remove enzymes and adapter dimers, and the final “SMRT bells” was eluted in 10 µl EB. Final quantification was carried out on an Agilent 2100 Bioanalyzer with 1 µl of library.

PacBio sequencing. The diluted library was loaded onto the instrument, along with DNA Sequencing Kit 2.0 (Part Number 100-216-400) and a SMRT Cell 8Pac. In all sequencing runs, 90 min movies were captured for each SMRT Cell loaded with a single binding complex. Primary filtering analysis was performed with the RS instrument and the secondary analysis was used the SMRT analysis pipeline version 2.1.0.

Illumina sequencing. Illumina library was sequenced on Hiseq X ten. Trimmomatic was used to trim adaptor, low quality base ($Q < 20$) and short reads (length < 50 bp).

Gene prediction and annotation

AUGUSTUS [35] and SNAP [36] were performed to predict coding genes. Genome functional annotation was performed using BLASTP, as well as NCBI non-redundant (NR), SwissProt, and Protein Information Resource (PIR) protein databases. All predicted genes were classified according to the Kyoto Encyclopedia of Genes and Genomes (KEGG) metabolic pathways and Cluster of Orthologous Groups of proteins (COG).

Prediction of secondary metabolites

To predict secondary metabolite biosynthesis of strain *M. purpureus* CSU-M183, the BGCs of secondary metabolites were annotated using antiSMASH fungi version 5.1.0 [37].

RT-qPCR analysis

RT-qPCR was performed according to the method described by Liu et al. [21], with β -Actin as the reference gene, the genes on the MPs and citrinin gene cluster were selected, and the expression of these genes was detected by qRT-PCR during the submerged fermentation of *M. purpureus* LQ-6 and *M. purpureus* CSU-M183, respectively. For removal of residual genomic DNA, RNA samples were treated with RNase-free DNaseI (Thermo Fisher Scientific, Massachusetts, USA) following the manufacturer’s protocol. The first-strand cDNA was synthesized using oligo-dT primers and EasyScript Reverse Transcriptase (TransGen Biotech, Beijing, China), according to the manufacturer’s protocol. qRT-PCR was performed using the TransStartGreen qPCR SuperMix UDG (TransGen Biotech, Beijing, China) according to the manufacturer’s instructions. $2^{-\Delta\Delta CT}$ was used to determine expression levels of the tested genes. The primers used in these analyses were listed in S1 Table.

Data availability

The assembled genome sequence of *M. purpureus* CSU-M183 has been deposited into the NCBI Genbank database with an accession number of JAACNI000000000. The BioProject and BioSample information are available at PRJNA599556 and SAMN13759458, respectively. The raw sequence data of *M. purpureus* CSU-M183 has been deposited into the NCBI Genbank database with an BioProject of PRJNA824977.

Ethical approval

This article does not contain any studies with human participants or animals performed by any of the authors.

Statistical analysis

Each experiment was performed at least in triplicate and the results are shown as the mean \pm standard deviation (SD). Statistical analyses were performed using the SPSS Statistics 23 (SPSS, Chicago, USA). Data were analyzed by one-way ANOVA, and tests of significant differences were determined by using Tukey multiple comparison or Student's t-test at $P < 0.05$.

Results and discussion

Overview of WGS

In the previous study, we obtained a high pigment-producing *M. purpureus* CSU-M183 strain using the ARTP mutation system [32]. The morphological characteristics of *Monascus* are closely related to the production of secondary metabolites in SF. To further study the metabolic engineering of the morphology of *M. purpureus* CSU-M183, the WGS of strain *M. purpureus* CSU-M183 was carried out. BUSCO analysis indicated 92% completeness based on fungi reference genes. Among the 290 BUSCO groups searched, 280 BUSCO groups (including complete and fragmented BUSCOs) were identified, occupying 96.5% of the total BUSCO groups. Among them, 267 groups were complete BUSCO groups, occupying 92.0% of the total BUSCO groups. The *M. purpureus* CSU-M183 genome sequence of 23.75 Mb was generated by assembling approximately 9.25 Gb raw data (353 \times coverage), which had a GC content of 49.13% and 69 genomic contigs (Table 1). The genome functional prediction and annotation identified 7305 protein-coding genes, with an average gene length of 1693 bp.

To investigate the functions of the coding genes and metabolic pathways, all coding sequences (CDSs) were subjected to COG and KEGG analysis [38]. The COG database (<http://www.ncbi.nlm.nih.gov/COG>) classifies proteins by comparing all protein sequences in the genome [39]. In total, 4157 CDSs were allocated to COG categories (Table 2), with the maximum proportion of sequences related to “carbohydrate transport and metabolism” (8.52%), followed by “amino acid transport and metabolism” (7.82%), “translation, ribosomal structure and biogenesis” (6.90%), “posttranslational modification, protein turnover, and chaperones” (6.88%), and “energy production and conversion” (5.08%). Proteins that have not been fully

Table 1. *M. purpureus* CSU-M183 genome general features.

Job Metric	Value
Length of genome assembly (Mb)	23.75 (23,752,195 bp)
Contig number	69
G + C content (%)	49.4
Coverage	353X
Q30 (%)	87.1
SNP number	3
Number of protein-coding genes	7305
Average gene length (bp)	1693
Genes with function prediction	5182
Number of proteins with KEGG ortholog	3362
Number of proteins with COG	4157

<https://doi.org/10.1371/journal.pone.0263905.t001>

Table 2. COG classification of predicted genes encoding proteins with annotated functions of *M. purpureus* CSU-M183 genome.

COG classification	Percentage(%)
RNA processing and modification	0.77
Chromatin structure and dynamics	0.77
Energy production and conversion	5.08
Cell cycle control, cell division, chromosome partitioning	2.98
Amino acid transport and metabolism	7.82
Nucleotide transport and metabolism	2.38
Carbohydrate transport and metabolism	8.52
Coenzyme transport and metabolism	4.04
Lipid transport and metabolism	4.38
Translation, ribosomal structure and biogenesis	6.90
Transcription	3.66
Replication, recombination and repair	4.40
Cell wall/membrane/envelope biogenesis	3.03
Cell motility	0.24
Posttranslational modification, protein turnover, chaperones	6.88
Inorganic ion transport and metabolism	3.80
Secondary metabolites biosynthesis, transport and catabolism	4.23
General function prediction only	19.08
Function unknown	4.81
Signal transduction mechanisms	2.36
Intracellular trafficking, secretion, and vesicular transport	2.02
Defense mechanisms	0.99
Nuclear structure	0.10
Cytoskeleton	0.77

<https://doi.org/10.1371/journal.pone.0263905.t002>

identified in the genome of strain CSU-M183 were classified as “general function prediction only” (19.08%) and “function unknown” (4.81%) in COG categories.

KEGG enrichment analysis is essential for understanding the complex biological functions of genes in microorganisms, including metabolic pathways, genetic information transfer, and cytological processes [40]. Altogether, 3362 CDSs were allocated to five categories in the KEGG database, including “metabolism”, “cellular process” and “environmental information processing”, “genetic information processing”, and “organismal systems” (Fig 1). Annotation results showed that “metabolism” is the main category of KEGG annotations (1375, 40.90%), followed by “genetic information processing” (707, 21.03%) and “organismal systems” (519, 15.44%). Moreover, CDSs were significantly enriched in “translation” (282), “carbohydrate metabolism” (279), “amino acid metabolism” (266) and “transport and catabolism” (259) sub-categories, indicating that *M. purpureus* CSU-M183 had the strong ability of protein translation, carbohydrate utilization and energy conversion.

Identification of secondary metabolites BGCs

AntiSMASH is a widely used tool that can identify and annotate BGCs in bacterial and fungal genome sequences [41]. To further understand the biosynthesis of the secondary metabolites in strain *M. purpureus* CSU-M183, BGCs prediction of secondary metabolites were performed using antiSMASH fungi version 5.1.0. A total of 26 BGCs were detected, including terpene,

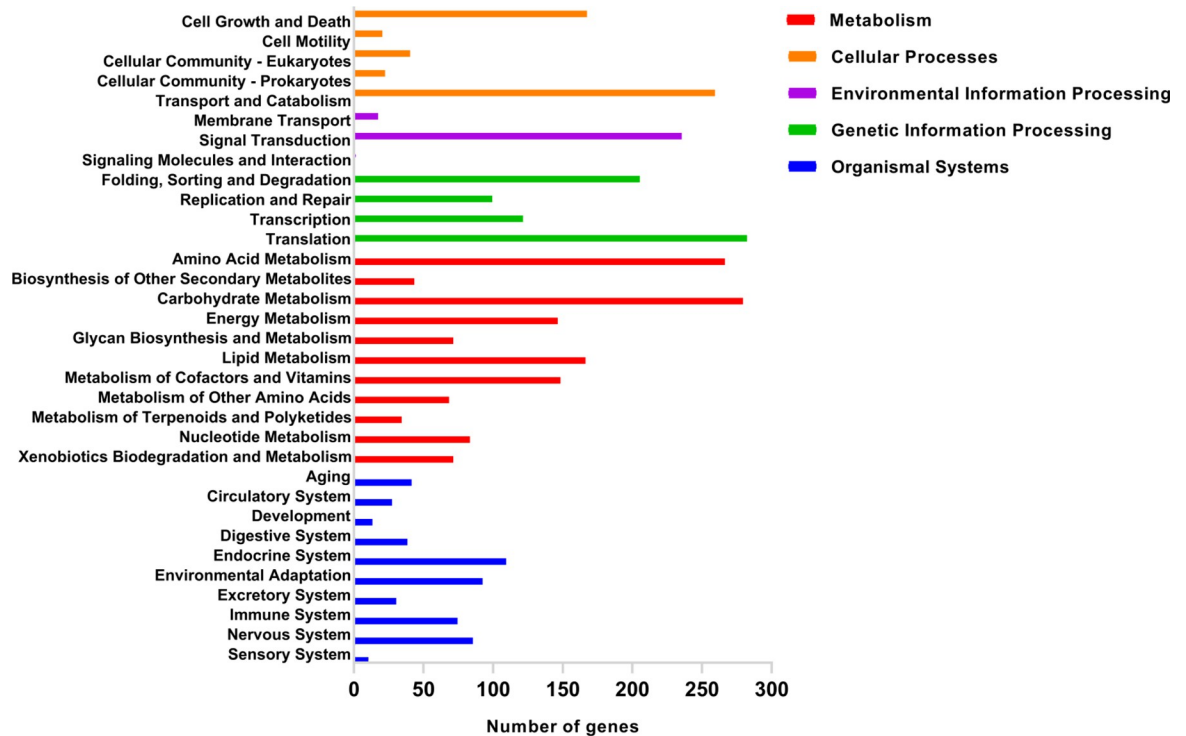


Fig 1. Enrichment analysis of KEGG pathways for predicted genes of the *M. purpureus* CSU-M183 genome. The y-axis represents the KEGG pathway and the x-axis denotes the number of genes.

<https://doi.org/10.1371/journal.pone.0263905.g001>

non-ribosomal peptide synthetases (NRPS), type I polyketide synthases (T1PKS), β -lactone, and 18 putative gene clusters.

After the database search with antiSMASH, a BGC (contig 000002F, gene g3398-g3411) for citrinin within the genome sequence of strain CSU-M183 was predicted (Fig 2A), which was identical to the known citrinin BGC (GenBank accession number: AB243687.1, 21917 bp) [42], and the identity of homologous genes was 99%-100%, the predicted functions of the genes in citrinin BGC are listed in Table 3. Additionally, 81% of homologous genes were similar to those in citrinin BGC0001338, and 57% in citrinin BGC000894. A putative BGC responsible for the biosynthesis of MPs was identified in the genome of strain CSU-M183 with 41% of homologous genes showed similar to that in BGC0000027 (Fig 2B), including 16 genes (contig 000001F, gene g1401-g1416) listed in Table 4. As shown in Table 4, the identity of homologous genes was considerably high, such as gene g1409 was 96.51% similar to *MpigA* (Polyketide synthase), gene g1407 was 95.05% similar to *MpigC* (Ketoreductase), and gene g1406 was 95.82% similar to *MpigD* (Acyltransferase). Moreover, by using the known monacolin K BGC (GenBank accession number: DQ176595.1, 45000 bp) of *M. pilosus* as a reference [13], no complete monacolin K BGC was detected in the genome sequence of *M. purpureus* CSU-M183 (Fig 2C). All protein-coding genes in the genome sequence were analyzed by BLASTP, where gene g3061, g2167, g4491, g1403, g1402, g4228, g1429, g1395 were homologous to the genes *mkA*~*mkL*, respectively. However, these genes do not locate in a gene cluster in genome, and the homologous protein identities were low, especially gene g1403 (with *mokD* of *M. pilosus* with 25.00% identity) (Table 5). It has been reported that overexpression of *mokD* significantly enhanced the production of monacolin K by 200.8%, which illustrated this gene play a vital role in the synthesis of monacolin K [24]. These findings were similar to that of the parent strain *M. purpureus* LQ-6, which could not produce monacolin K [43].

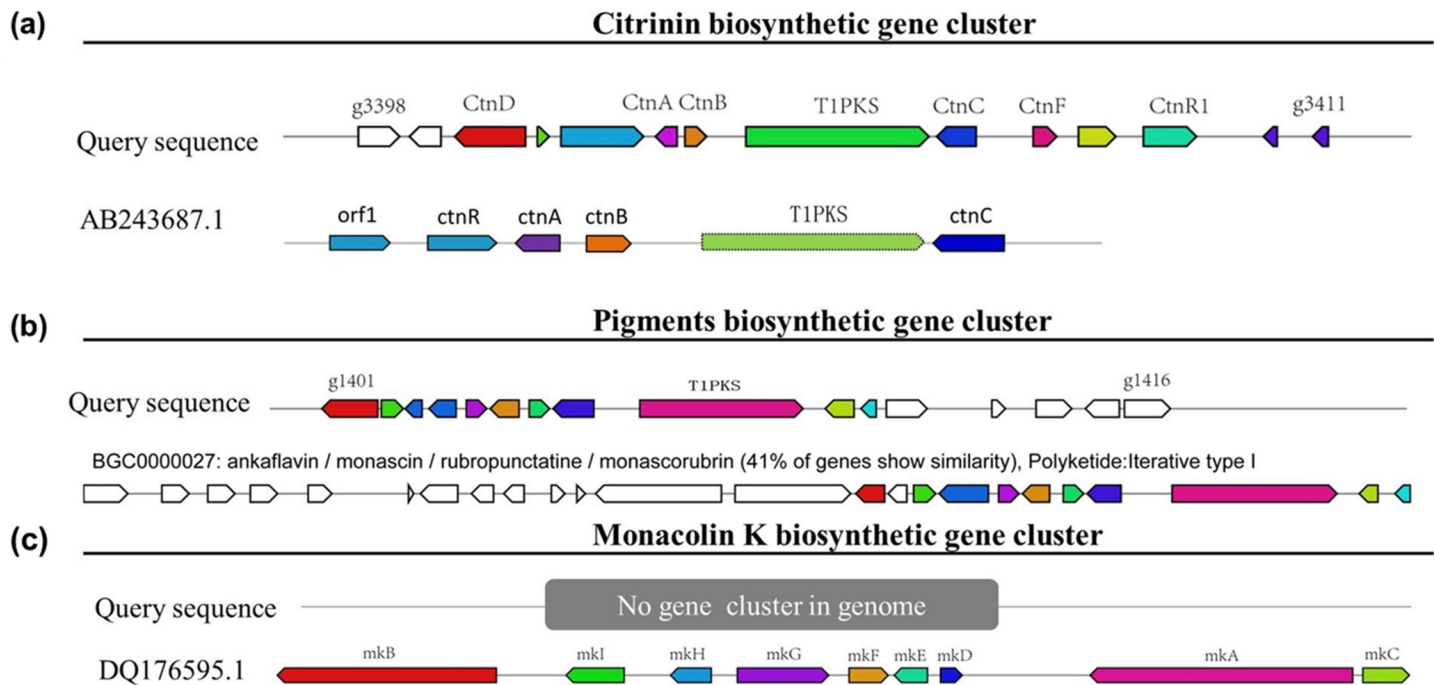


Fig 2. Schematic representation of predominant secondary metabolites BGCs in the genome sequence of *M. purpureus* CSU-M183. (a) Citrinin. (b) MPs. (c) Monacolin K.

<https://doi.org/10.1371/journal.pone.0263905.g002>

Due to various species of *Monascus* and large gaps in available biological information, the development of basic theoretical research on *Monascus* has been relatively slow. With the continuous development of sequencing technology and bioinformatics, breakthrough progress has been made in biosynthetic pathways of the secondary metabolites of *Monascus* [19, 44, 45], among which MPs, citrinin and monacolin K are the most notable. However, studies on functional and comparative genomics—such as the annotation of unknown sequences, investigation of gene models, comparison of multiple sequence alignment analysis, and metabolic

Table 3. Functional prediction of genes detected in the citrinin BGC of *M. purpureus* CSU-M183.

CDS	Length (bp)	Product	KO
gene = g3398	1762	Unnamed protein product	
gene = g3399	1389	Hypothetical protein, <i>orf7</i>	
gene = g3400	2796	<i>ctnD</i>	K00108
gene = g3401	403	Predicted protein	K00108
gene = g3402	3076	Dehydrogenase, <i>orf1</i>	
gene = g3403	987	citrinin biosynthesis oxygenase, <i>ctnA</i>	K13821
gene = g3404	940	citrinin biosynthesis oxydoreductase, <i>ctnB</i>	
gene = g3405	7780	citrinin polyketide synthase, <i>pksCT</i>	
gene = g3406	1497	citrinin biosynthesis transporter, <i>ctnC</i>	
gene = g3407	829	<i>ctnF</i>	
gene = g3408	1498	Hypothetical protein, <i>orf8</i>	
gene = g3409	2116	<i>ctnR</i>	
gene = g3410	663	<i>ctnG</i>	
gene = g3411	567	<i>ctnG</i>	K01673
gene = g3412	3163	<i>ctnI</i>	

<https://doi.org/10.1371/journal.pone.0263905.t003>

engineering of *Monascus* morphology, which can elaborate the relationship among secondary metabolite productivity, growth, and morphology in SF, are less.

The key gene PKS with 7838 bp responsible for citrinin biosynthesis was first identified from *M. purpureus* in 2005 [46] and then five genes encoding Zn(II)₂Cys₆ transcriptional activator, membrane transporter, dehydrogenase, oxygenase, and oxidoreductase for citrinin biosynthesis were cloned [47]. Microbial PKSs have been mainly classified into three types—type I PKSs (modular type I PKSs and iterative type I PKSs), type II PKSs, and type III PKSs. The PKS responsible for citrinin biosynthesis belongs to the iterative type I PKSs, which contains putative domains for ketosynthase (KS), acyltransferase (AT), ketoreductase (KR), dehydratase (DH), enoyl reductase (ER), methyltransferase (MT), thioesterase (TE), and acyl carrier protein (ACP) [46]. The KS domain catalyzes the condensation of precursors to extend the polyketone chain, whereas the AT domain selects the precursors, and the ACP domain makes covalent bonds between the precursors and intermediates, which are necessary for the functioning of most PKSs [48]. In 2012, the citrinin BGC with the length of 43 kb from *Monascus aurantiacus* was first published [49], including 16 open reading frames (ORFs) for *ctnD*, *ctnE*, *orf6*, *orf1*, *ctnA*, *orf3*, *orf4*, *pkcCT*, *orf5*, *ctnF*, *orf7*, *ctnR*, *orf8*, *ctnG*, *ctnH*, and *ctnI*, which are dramatically similar to those of the citrinin BGC of strain *M. purpureus* CSU-M183. These results revealed high homology of citrinin BGC in *Monascus*, especially the key gene PKS. In 2012, a putative 53 kb MP BGC of *M. ruber* was first reported, which consisted of genes encoding PKSs, fatty acid synthases, regulatory factors, and dehydrogenase [3]. Xie et al. reported that gene *pigR* (gene g1401 in Table 4) is a positive regulatory gene in MPs biosynthesis pathway [50], whereas gene *MpigE* (gene g1402 in Table 4) may be involved in the conversion of different MPs [51]. The genome size of *M. purpureus* was found to be smaller than that of related filamentous fungi, indicating a significant loss of genes [19]. A previous study reported that monacolin K cannot be produced due to the lack of monacolin K biosynthesis locus in some *M. purpureus* genomes [52]. After the prediction of monacolin K BGC in the genome of strain CSU-M183, we found that there was no complete monacolin K BGC in the strain CSU-M183, which was consistent with previous studies [43, 52]. Undoubtedly, the identification of BGCs has greatly facilitated the understanding of the biosynthetic pathways of

Table 4. Functional prediction of genes detected in the MPs BGC of *M. purpureus* CSU-M183.

CDS	Length (bp)	Product	Identity (%)	KO
gene = g1401	2388	Fungal specific transcription factor, <i>MpigR</i>	91.41	
gene = g1402	1108	Alcohol dehydrogenase, <i>MpigE</i>	95.39	
gene = g1403	819	Amino oxidase/esterase, <i>MpigF</i>	93.01	
gene = g1404	1395	Amino oxidase/esterase, <i>MpigF</i>	94.03	
gene = g1405	1027	Dehydrogenase, <i>MpigH</i>	97.66	
gene = g1406	1449	Acyltransferase, <i>MpigD</i>	95.82	K22889
gene = g1407	892	Ketoreductase, <i>MpigC</i>	95.05	K11165
gene = g1408	1719	Citrinin biosynthesis transcriptional activator <i>CtnR</i>	95.48	
gene = g1409	8071	Polyketide synthase, <i>MpigA</i>	96.51	
gene = g1410	1032	Peptidyl-prolyl cis-trans isomerase <i>Cpr7</i>	98.68	K05864
gene = g1411	573	D-tyrosyl-tRNA(Tyr) deacylase, <i>MpigO</i>	95.58	K07560
gene = g1412	1849	TPA: CCR4-NOT transcription complex, subunit 3	84.23	K12580
gene = g1413	634	C ₂ H ₂ finger domain protein	76.40	
gene = g1414	1531	Dihydrolipoamide dehydrogenase	84.17	K00382
gene = g1415	1665	Fatty acid desaturase	73.58	K13076
gene = g1416	1792	Phosphoglucomutase	68.45	K01835

<https://doi.org/10.1371/journal.pone.0263905.t004>

Table 5. Functional prediction of genes detected in the monacolin K BGC of *M. purpureus* CSU-M183 by NCBI-BLASTP.

CDS	Length (aa)	Homologue	Homologue Length (aa)	Identity
gene = g3061	3945	ABA02239.1_8 [gene = mkA]	3075	37.19%
gene = g2167	2593	ABA02240.1_1 [gene = mkB]	2547	38.62%
gene = g4491	499	ABA02241.1_9 [gene = mkC]	524	80.53%
gene = g1403	273	ABA02242.1_7 [gene = mkD]	263	25.00%
gene = g1402	369	ABA02243.1_6 [gene = mkE]	360	39.17%
gene = g4228	1133	ABA02245.1_4 [gene = mkG]	1052	52.61%
gene = g1429	426	ABA02246.1_3 [gene = mkH]	455	78.10%
gene = g1395	570	ABA02247.1_2 [gene = mkI]	543	54.21%

<https://doi.org/10.1371/journal.pone.0263905.t005>

secondary metabolites in *Monascus*, which can provide theoretical support for industrial production of *Monascus* secondary metabolites.

Expression level of *Monascus* pigments and citrinin clusters located genes

After 7 days of SF, the MPs and citrinin yields of *M. purpureus* LQ-6 and *M. purpureus* CSU-M183 were 43.97 U/ml, 1.27 mg/L and 83.77 U/ml, 5.34 mg/L, respectively (Fig 3A). To verify the effect of mutagenesis on the metabolism of MPs and citrinin, the relative expression levels of several key genes, *MpigA*, *MpigR*, *MpigC*, *MpigD*, *MpigE*, *MpigF*, *MpigG*, *MpigH*, *MpigI*, *MpigJ*, *MpigK*, *MpigL*, *MpigM*, *MpigP*, *MpigQ*, *cit S*, *cit A*, *cit B*, *cit C*, *cit D* and *cit E* were investigated using RT-qPCR. As shown in Fig 3B and 3C, the relative expression levels of *MpigM*, *MpigP*, *cit B*, *cit C*, *cit D* and *cit E* in *M. purpureus* CSU-M183 were extremely significant ($p < 0.001$) compared to that of *M. purpureus* LQ-6 at 4th day; while the relative expression levels of *MpigA*, *MpigJ*, *MpigK*, *cit S*, *cit C* in *M. purpureus* CSU-M183 were extremely significant ($p < 0.001$) than that of *M. purpureus* LQ-6 at 7th day. During the fermentation process, in addition to the relative expression of extremely significant ($p < 0.001$) genes, the expression levels of other genes in the MPs and citrinin biosynthesis gene clusters in CSU-M183 were very significant ($p < 0.01$), such as *MpigA*, *MpigC*, *MpigD*, *MpigF*, *MpigG* and *cit S* at 4th day and *MpigD*, *MpigG*, *MpigH* and *cit B* at 7th day. The production of MPs and citrinin is directly or indirectly related to the function of genes in their biosynthetic gene clusters, and the relative expression of genes can directly reflect the contribution of genes in the fermentation process. A number of studies have performed functional analysis of MPs and citrinin gene clusters, such as: inactivating *MpigA* in *M. ruber*, *Monascus* lost its pigment production ability, which proved that PKS was involved in pigment synthesis [53]. *MrpigI*(encoded by *MrpigI*, a homolog of *MpigI*) and *MrpigK*(encoded by *MrpigK*, a homolog of *MpigK*) form two subunits of the specialized fungal FAS, which produce the fatty acyl portion of the side chain of MPs [54]. Moreover, *MrpigM*, as an o-acetyltransferase, synthesized an O-11 acetyl intermediate in Chen et al's *Monascus* model, and knocking out *MrpigM*(the homolog of *MpigM*) blocked the pathway of pigment synthesis intermediate [54]. The inactivation of genes in citrinin biosynthesis gene cluster led to a significant decline on citrinin production, even lower than the detection level, such as knocking out *cit A*, *pksCT* and *cit B* [42, 55]. It indicates that the increase of MPs and citrinin production may be caused by the increase of gene expression level in gene cluster caused by ARTP mutation, and these genes are very important for the synthesis of MPs and citrinin.

Analysis of the chitin biosynthesis pathway

As the main component of the fungal cell wall, chitin is important for the morphology of fungi. Based on the homology of amino acid sequence, chitin synthetases can be divided into

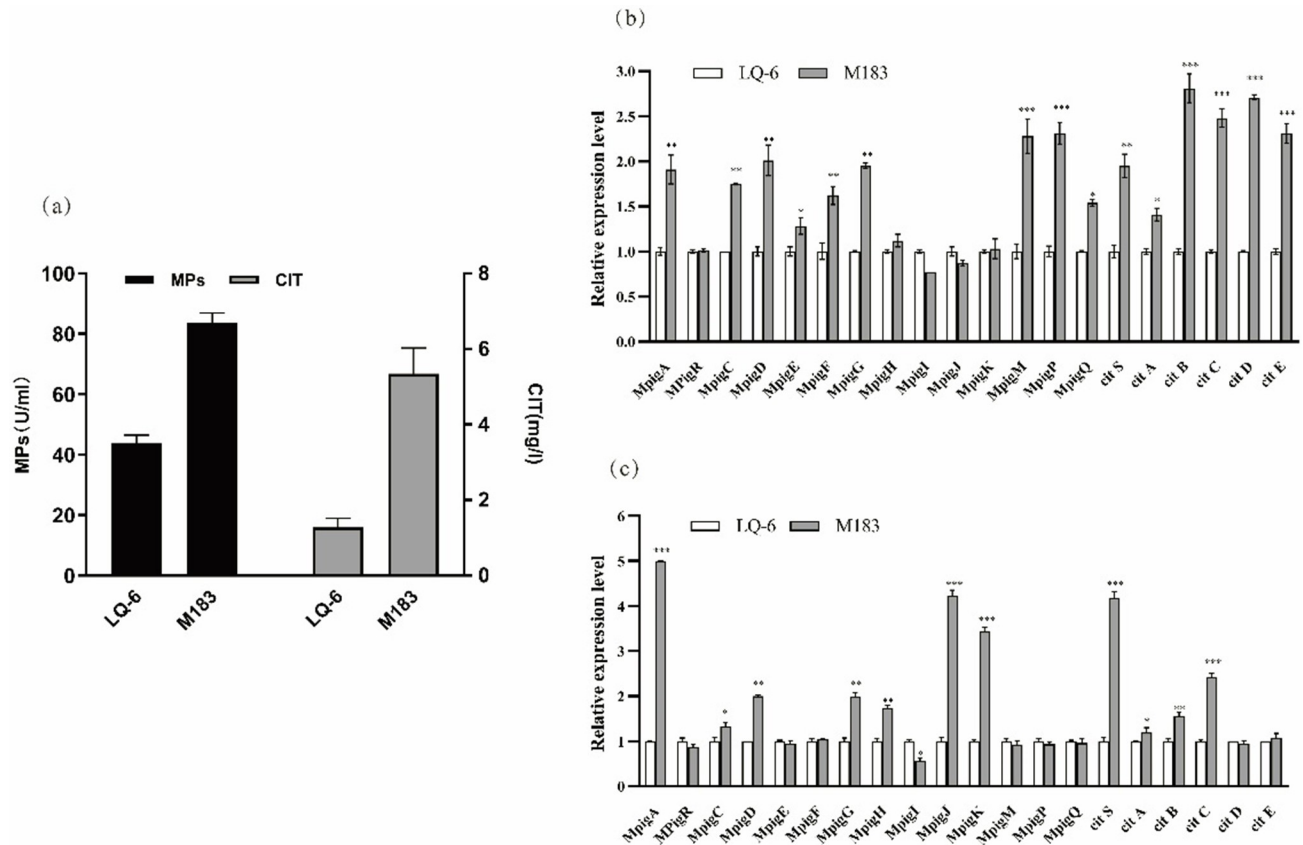


Fig 3. (a) Production of MPs and citrinin in SF of *M. purpureus* LQ-6 and *M. purpureus* CSU-M183 for 7 days. (b) Expression levels of genes related to MPs and citrinin biosynthesis of *M. purpureus* LQ-6 (control) and *M. purpureus* CSU-M183 at 4th day. (c) Expression levels of genes related to MPs and citrinin biosynthesis of *M. purpureus* LQ-6 (control) and *M. purpureus* CSU-M183 at 7th day. * $p < 0.05$, ** $p < 0.01$, *** $p < 0.001$.

<https://doi.org/10.1371/journal.pone.0263905.g003>

three categories (class I-III) in *Saccharomyces cerevisiae*, four (class I-IV) in *Candida albicans*, and seven (class I-VII) in filamentous fungi. The numbers of gene encoding chitin synthetase in various filamentous fungi are different, generally containing 6–10 genes encoding chitin synthetase [56].

To date, information about chitin biosynthesis in *M. purpureus* has not been reported. To lay a foundation for the further study of morphological metabolism of *M. purpureus*, we analyzed the chitin biosynthesis of strain CSU-M183 and annotated the function of the relevant genes in the pathway. By matching the predicted chitin biosynthesis-related enzymes in CSU-M183 strain genome with the KEGG database, the biosynthetic pathway of chitin in *M. purpureus* was identified. As shown in Fig 4, phosphoacetylglucosamine mutase (PGM3) [EC:5.4.2.3] (encoded by gene g4907) converts N-acetyl-D-glucosamine 6-phosphate (GlcNAc-6P) to N-acetyl-alpha-D-glucosamine 1-phosphate (GlcNAc-1P), which is then dephosphorylated by UDP-N-acetylglucosamine diphosphorylase (UAP1) [EC:2.7.7.23] (encoded by gene g6630) to yield UDP-N-acetyl-D-glucosamine (UDP-GlcNAc). Moreover, chitin synthase (*chs1*) [EC:2.4.1.16] (encoded by genes: g872, g920, g3078, and g5640) converts UDP-GlcNAc to chitin. Additionally, the other genes encoding the important enzymes in the biosynthetic pathway of chitin were annotated, such as N-acetylmuramic acid 6-phosphate etherase (*murQ*) [EC:4.2.1.126] encoded by gene g1905, chitinase [EC:3.2.1.14] encoded by genes g3222, g6372 and g1142, and glucosamine-phosphate N-acetyltransferase (GNPNAT1, GNA1) [EC:2.3.1.4] encoded by gene g2832.

Conclusion

Genomic information of *M. purpureus* CSU-M183 reported here can serve as a reference genome for *Monascus* genomics research. It's predicted that the secondary metabolites BGCs and the chitin biosynthetic pathway in the genome of *M. purpureus* CSU-M183. We verified that ARTP induced significantly the upregulated expression of most *Monascus* pigment and citrinin clusters located genes by RT-qPCR. In addition, we annotated and classified the chitin biosynthesis genes of *M. purpureus* CSU-M183, which offer a strategy of morphological metabolic engineering. In conclusion, we provided genomic resources for further biological studies on the metabolic engineering of the morphology of *Monascus*.

Supporting information

S1 Table. The primers used in this study.
(DOCX)

Acknowledgments

We would like to thank Editage for English language editing.

Author Contributions

Data curation: Jun Liu.

Formal analysis: Song Zhang.

Methodology: Xiaofang Zeng.

Resources: Qinlu Lin.

Writing – original draft: Song Zhang.

Writing – review & editing: Jun Liu.

References

1. Patakova P. *Monascus* secondary metabolites: production and biological activity. *Journal of Industrial Microbiology & Biotechnology*. 2013; 40(2):169–81. <https://doi.org/10.1007/s10295-012-1216-8> PMID: 23179468
2. Kim D, S K. Beneficial effects of *Monascus* sp. KCCM 10093 pigments and derivatives: A mini review. *Molecules*. 2018; 23(1):98. <https://doi.org/10.3390/molecules23010098> PMID: 29301350
3. Feng YL, Shao YC, Cheng FS. *Monascus* pigments. *Applied Microbiology & Biotechnology*. 2012; 96:1421–1440. <https://doi.org/10.1007/s00253-012-4504-3> PMID: 23104643
4. Chen G, Yang S, Wang C, Shi K, Wu Z. Investigation of the mycelial morphology of *Monascus* and the expression of pigment biosynthetic genes in high-salt-stress fermentation. *Applied Microbiology and Biotechnology*. 2020; 104(6):2469–79. <https://doi.org/10.1007/s00253-020-10389-2> PMID: 31993704
5. Downham A, Collins P. Colouring our foods in the last and next millennium. *International Journal of Food ence & Technology*. 2010; 35(1):5–22.
6. Zhao L, Lu F, Zhang X, Wang Z. Isolation of ionizable red *Monascus* pigments after extractive fermentation in nonionic surfactant micelle aqueous solution. *Process Biochemistry*. 2017; 61:156–62.
7. Liu J, Luo Y, Guo T, Tang C, Lin Q. Cost-effective pigment production by *Monascus purpureus* using rice straw hydrolysate as substrate in submerged fermentation. *Journal of Bioscience and Bioengineering*. 2019; 129(2):229–236. <https://doi.org/10.1016/j.jbiosc.2019.08.007> PMID: 31500988
8. Wang Y, Zhang B, Lu L, Huang Y, Xu G. Enhanced production of pigments by addition of surfactants in submerged fermentation of *Monascus purpureus* H1102. *Journal of the Science of Food & Agriculture*. 2013; 93(13):3339–44. <https://doi.org/10.1002/jsfa.6182> PMID: 23595359

9. Lin L, Wang C, Li Z, Wu H, Chen M. Effect of Temperature-Shift and Temperature-Constant Cultivation on the Monacolin K Biosynthetic Gene Cluster Expression in *Monascus* sp. *Food Technology and Biotechnology*. 2017; 55(1):40. <https://doi.org/10.17113/ftb.55.01.17.4729> PMID: 28559732
10. Lin L, Wu S, Li Z, Ren Z, Wang C. High Expression Level of mok E Enhances the Production of Monacolin K in *Monascus*. *Food Biotechnology*. 2018; 32(1):35–46.
11. Huang J, Liao NQ, Li HM. Linoleic acid enhance the production of moncolin K and red pigments in *Monascus ruber* by activating mokH and mokA, and by accelerating cAMP-PkA pathway. *International Journal of Biological Macromolecules: Structure, Function and Interactions*. 2018; 109:950–4.
12. Zhang, BB, Xing, Hong-Bo, Jiang, Bing-Jie, et al. Using millet as substrate for efficient production of monacolin K by solid-state fermentation of *Monascus ruber*. *Journal of Bioscience and Bioengineering*. 2017; 125(3):333–338. <https://doi.org/10.1016/j.jbiosc.2017.10.011> PMID: 29157871
13. Chen YP, Yuan GF, Hsieh SY, Lin YS, Wang WY, Liaw LL, et al. Identification of the *mokH* gene encoding transcription factor for the upregulation of Monacolin K biosynthesis in *Monascus pilosus*. *Journal of Agricultural and Food Chemistry*. 2010; 58(1):287–93. <https://doi.org/10.1021/jf903139x> PMID: 19968298
14. Feng Y, Chen W, Chen F. A *Monascus pilosus* MS-1 strain with high-yield monacolin K but no citrinin. *Food Science & Biotechnology*. 2016; 25(4):1115–22. <https://doi.org/10.1007/s10068-016-0179-3> PMID: 30263383
15. Simu SY, Castro-Aceituno V, Lee S, Ahn S, Lee HK, Hoang VA, et al. Fermentation of soybean hull by *Monascus pilosus* and elucidation of its related molecular mechanism involved in the inhibition of lipid accumulation. An in silico and in vitro approach. *Journal of Food Biochemistry*. 2018; 42(1): e12442.
16. Embaby AM, Hussein MN, Hussein A, Papp T. *Monascus* orange and red pigments production by *Monascus purpureus* ATCC16436 through co-solid state fermentation of corn cob and glycerol: An eco-friendly environmental low cost approach. *Plos One*. 2018; 13(12):e0207755. <https://doi.org/10.1371/journal.pone.0207755> PMID: 30532218
17. Lv J, Qian GF, Chen L, Liu H, Xu HX, Xu GR, et al. Efficient Biosynthesis of Natural Yellow Pigments by *Monascus purpureus* in a Novel Integrated Fermentation System. *Journal of Agricultural and Food Chemistry*. 2018; 66(4):918–925. <https://doi.org/10.1021/acs.jafc.7b05783> PMID: 29313328
18. Suraiya S, Siddique MP, Lee JM, Kim EY, Kim JM, Kong IS. Enhancement and characterization of natural pigments produced by *Monascus* spp. using *Saccharina japonica* as fermentation substrate. *Journal of Applied Phycology*. 2017; 30:729–742.
19. Yang Y, Liu B, Du XJ, Li P, Liang B, Cheng XZ, et al. Complete genome sequence and transcriptomics analyses reveal pigment biosynthesis and regulatory mechanisms in an industrial strain, *Monascus purpureus* YY-1. *Sci Rep*. 2015; 5:8331. <https://doi.org/10.1038/srep08331> PMID: 25660389
20. Kumagai T, Tsukahara M, Katayama N, Yaoi K, Fujimori KE. Whole-Genome Sequence of *Monascus purpureus* GB-01, an Industrial Strain for Food Colorant Production. *Microbiology Resource Announcements*. 2019; 8(24): e00196–19. <https://doi.org/10.1128/MRA.00196-19> PMID: 31196916
21. Liu J, Chai XY, Guo T, Wu JY, Yang PP, Luo YC, et al. Disruption of the Ergosterol Biosynthetic Pathway Results in Increased Membrane Permeability, Causing Overproduction and Secretion of Extracellular *Monascus* Pigments in Submerged Fermentation. *Journal of Agricultural and Food Chemistry*. 2019; 67(49):13673–83. <https://doi.org/10.1021/acs.jafc.9b05872> PMID: 31617717
22. Chen G, Huang T, Bei Q, Tian XF, Wu ZQ. Correlation of pigment production with mycelium morphology in extractive fermentation of *Monascus anka* GIM 3.592. *Process Biochemistry*. 2017; 58:42–50.
23. Lv J, Zhang BB, Liu XD, Zhang C, Chen L, Xu GR, et al. Enhanced production of natural yellow pigments from *Monascus purpureus* by liquid culture: The relationship between fermentation conditions and mycelial morphology. *Journal of Bioscience and Bioengineering*. 2017:452–8. <https://doi.org/10.1016/j.jbiosc.2017.05.010> PMID: 28625612
24. Zhang C, Liang J, Zhang A, Hao S, Zhang H, Zhu Q, et al. Overexpression of Monacolin K Biosynthesis Genes in the *Monascus purpureus* Azaphilone Polyketide Pathway. *Journal of Agricultural and Food Chemistry*. 2019; 67(9):2563–69. <https://doi.org/10.1021/acs.jafc.8b05524> PMID: 30734557
25. Ibrahim D, Weloosamy H, Lim SH. Effect of agitation speed on the morphology of *Aspergillus niger* HFD5A-1 hyphae and its pectinase production in submerged fermentation. *World Journal of Biological Chemistry*. 2015; 6(3): 265–71. <https://doi.org/10.4331/wjbc.v6.i3.265> PMID: 26322181
26. Sun XW, Wu HF, Zhao GH, Li ZM, Wu XH, Liu H, et al. Morphological regulation of *Aspergillus niger* to improve citric acid production by *chsC* gene silencing. *Bioprocess and Biosystems Engineering*. 2018; 41(7): 1029–1038. <https://doi.org/10.1007/s00449-018-1932-1> PMID: 29610994
27. Calvo AM. The *VeA* regulatory system and its role in morphological and chemical development in fungi. *Fungal Genetics and Biology*. 2008; 45(7):1053–61. <https://doi.org/10.1016/j.fgb.2008.03.014> PMID: 18457967

28. Tan YM, Wang H, Wang YP, Ge YY, Ren XX, Ren CG, et al. The role of the *veA* gene in adjusting developmental balance and environmental stress response in *Aspergillus cristatus*. *Fungal Biology*. 2018; 122(10):952–64. <https://doi.org/10.1016/j.funbio.2018.05.010> PMID: 30227931
29. Müller C, McIntyre M, Hansen K, Nielsen J. Metabolic engineering of the morphology of *Aspergillus oryzae* by altering chitin synthesis. *Applied & Environmental Microbiology*. 2002; 68(4):1827–36. <https://doi.org/10.1128/AEM.68.4.1827-1836.2002> PMID: 11916702
30. Liu H, Zheng Z, Wang P, Gong G, Wang L, Zhao G. Morphological changes induced by class III chitin synthase gene silencing could enhance penicillin production of *Penicillium chrysogenum*. *Applied Microbiology and Biotechnology*. 2013; 97(8):3363–72. <https://doi.org/10.1007/s00253-012-4581-3> PMID: 23179625
31. Lenardon M, Munro CA, Gow N. Chitin synthesis and fungal pathogenesis. *Current Opinion in Microbiology*. 2010; 13(4):416–23. <https://doi.org/10.1016/j.mib.2010.05.002> PMID: 20561815
32. Liu J, Guo T, Luo YC, Chai XY, Wu JY, Zhao W, et al. Enhancement of *Monascus* pigment productivity via a simultaneous fermentation process and separation system using immobilized-cell fermentation. *Bioresource Technology*. 2019; 272:552–560. <https://doi.org/10.1016/j.biortech.2018.10.072> PMID: 30396112
33. Simão SF, Waterhouse RM, Panagiotis I, Kriventseva EV, Zdobnov EM. BUSCO: assessing genome assembly and annotation completeness with single-copy orthologs. *Bioinformatics*. 2015; 31(19):3210–2. <https://doi.org/10.1093/bioinformatics/btv351> PMID: 26059717
34. Vasanthan J, Yasubumi S. Comprehensive evaluation of non-hybrid genome assembly tools for third-generation PacBio long-read sequence data. *Briefings in Bioinformatics*. 2019; 20(3):866–876. <https://doi.org/10.1093/bib/bbx147> PMID: 29112696
35. Stanke M, Schffmann O, Morgenstern B, Waack S. Gene prediction in eukaryotes with a generalized hidden Markov model that uses hints from external sources. *BMC Bioinformatics*. 2006; 7:62. <https://doi.org/10.1186/1471-2105-7-62> PMID: 16469098
36. Ian K. Gene finding in novel genomes. *BMC Bioinformatics*. 2004; 5(1):59.
37. Weber T, Blin K, Duddela S, Krug D, Kim HU, Brucoleri R, et al. antiSMASH 3.0—a comprehensive resource for the genome mining of biosynthetic gene clusters. *Nucleic Acids Research*. 2015; 43:W237–W243. <https://doi.org/10.1093/nar/gkv437> PMID: 25948579
38. Minoru K, Susumu G, Shuichi K, Yasushi O, Masahiro H. The KEGG resource for deciphering the genome. *Nucleic Acids Research*. 2004; 32:D277–D280. <https://doi.org/10.1093/nar/gkh063> PMID: 14681412
39. Tatusov RL, Galperin MY, Natale DA, Koonin EV. The COG database: a tool for genome-scale analysis of protein functions and evolution. *Nucleic Acids Research*. 2000;(1):33–6. <https://doi.org/10.1093/nar/28.1.33> PMID: 10592175
40. Xiang YP, Wang YM, Shen H, Wang DY. The Draft Genome Sequence of *Pseudomonas putida* Strain TGRB4, an Aerobic Bacterium Capable of Producing Methylmercury. *Current Microbiology*. 2020; 77(4): 522–527. <https://doi.org/10.1007/s00284-019-01670-3> PMID: 31004191
41. Kai B, Simon S, Katharina S, Rasmus V, Nadine Z, Yup LS, et al. antiSMASH 5.0: updates to the secondary metabolite genome mining pipeline. *Nuclc Acids Research*. 2019;(W1):W81–W87.
42. Xu MJ, Yang ZL, Liang ZZ, SN Z. Construction of a *Monascus purpureus* mutant showing lower citrinin and higher pigment production by replacement of *ctn A* with *pks 1* without using vector and resistance gene. *Journal of Agricultural and Food Chemistry*. 2009; 57(20):9764–8. <https://doi.org/10.1021/jf9023504> PMID: 20560630
43. Chai X, Ai Z, Liu J, Guo T, Bai J, Lin QL. Effects of pigment and citrinin biosynthesis on the metabolism and morphology of *Monascus purpureus* in submerged fermentation. *Food Science and Biotechnology*. 2020; 29(7):927–937. <https://doi.org/10.1007/s10068-020-00745-3> PMID: 32582455
44. Chen WP, He Y, Zhou Y, Shao YC, Chen FS. Edible filamentous fungi from the species *Monascus*: early traditional fermentations, modern molecular biology, and future genomics. *Comprehensive Reviews in Food Science & Food Safety*. 2015; 14(5):555–67.
45. Li L, Shao YC, Li Q, Yang S, Chen FS. Identification of *Mga1*, a G-protein α -subunit gene involved in regulating citrinin and pigment production in *Monascus ruber*M7. *Fems Microbiology Letters*. 2010; 308(2):108–14. <https://doi.org/10.1111/j.1574-6968.2010.01992.x> PMID: 20500530
46. Shimizu T, Kinoshita H, Ishihara S, Sakai K, Nagai S, T N. Polyketide synthase gene responsible for citrinin biosynthesis in *Monascus purpureus*. *Applied and Environmental Microbiology*. 2005. <https://doi.org/10.1128/AEM.71.7.3453-3457.2005> PMID: 16000748
47. Shimizu T, Kinoshita H, Nihira T. Identification and in vivo functional analysis by gene disruption of *ctnA*, an activator gene Involved in citrinin biosynthesis in *Monascus purpureus*. *Applied and Environmental Microbiology*. 2007; 73(16):5097. <https://doi.org/10.1128/AEM.01979-06> PMID: 17586673

48. Chen A, Schnarr N, Kim C, Cane D, Khosla C. Extender unit and acyl carrier protein specificity of ketosynthase domains of the 6-deoxyerythronolide B synthase. *Journal of the American Chemical Society*. 2006; 128(9):3067–74. <https://doi.org/10.1021/ja058093d> PMID: 16506788
49. Li YP, Yang X, Huang ZB. Isolation and characterization of the citrinin biosynthetic gene cluster from *Monascus aurantiacus*. *Biotechnology Letters*. 2012; 34(1):131–6. <https://doi.org/10.1007/s10529-011-0745-y> PMID: 21956130
50. Xie NN, Liu QP, Chen FS. Deletion of *pigR* gene in *Monascus ruber* leads to loss of pigment production. *Biotechnology Letters*. 2013; 35(9): 1425–32. <https://doi.org/10.1007/s10529-013-1219-1> PMID: 23690031
51. Liu QP, Xie NN, He Y, Wang L, Shao YC, Zhao HZ, et al. *MpigE*, a gene involved in pigment biosynthesis in *Monascus ruber* M7. *Applied Microbiology and Biotechnology*. 2014; 98(1):285–96. <https://doi.org/10.1007/s00253-013-5289-8> PMID: 24162083
52. Kwon HJ, Balakrishnan B, Kim YK. Some *Monascus purpureus* genomes lack the Monacolin K biosynthesis locus. *J. Appl. Biol. Chem*. 2016; 59(1):45–47.
53. Shao YC, Lei M, Mao ZJ, Zhou YX, Chen FS. Insights into *Monascus* biology at the genetic level. *Applied Microbiology and Biotechnology*. 2014; 98(9):3911–22. <https://doi.org/10.1007/s00253-014-5608-8> PMID: 24633442
54. Chen WP, Chen RF, Liu QP, He Y, He K, Ding XL, et al. Orange, red, yellow: biosynthesis of azaphilone pigments in *Monascus* fungi. *Chemical Science*. 2017; 8(7):4917–25. <https://doi.org/10.1039/c7sc00475c> PMID: 28959415
55. Li YP, Pan YF, Zou LH, Yang X, Huang ZB, He QH. Lower citrinin production by gene disruption of *ctnB* involved in citrinin biosynthesis in *Monascus aurantiacus* Li AS3.4384. *Journal of Agricultural and Food Chemistry*. 2013; 61(30):7397–402. <https://doi.org/10.1021/jf400879s> PMID: 23841779
56. Zhang JJ, Jiang H, Du YR, Keyhani NO, Xia YX, K J. Members of chitin synthase family in *Metarhizium acridum* differentially affect fungal growth, stress tolerances, cell wall integrity and virulence. *PLOS Pathog*. 2019; 15(8): e1007964. <https://doi.org/10.1371/journal.ppat.1007964> PMID: 31461507
57. Fukuda K, Yamada K, De Oka K, Yamashita S, Horiuchi H. Class III chitin synthase ChsB of *Aspergillus nidulans* localizes at the sites of polarized cell wall synthesis and is required for conidial development. *Eukaryotic Cell*. 2009; 8(7):945–56. <https://doi.org/10.1128/EC.00326-08> PMID: 19411617